

Axisymmetric Jet Control Using Passive Grids

R. Lehman, S. Rajagopalan, P. Burattini and R. A. Antonia

Discipline of Mechanical Engineering, School of Engineering
 The University of Newcastle, NSW, 2308 AUSTRALIA

Abstract

The structure of a circular jet, modified by placing grids of two different configurations near the nozzle exit plane, was investigated by using a single hot wire probe. An annular grid which perturbed mainly the axisymmetric shear layer and a circular disk grid which covered most of the potential core were used to modify the jet passively. Behind the annular mesh, the width of the shear layer is reduced and a significant decrease in turbulence intensity is observed. Spectra of the velocity fluctuation show the suppression of the formation of organised structures in the jet mixing layer. In contrast to the annular grid, the influence of the disk grid on the mean velocity and turbulence intensity is not as significant. Evidence for the presence of large scale structures downstream of the edges of the grids is presented.

Introduction

Turbulence control or management in different flows is a rapidly expanding field of research because of potential benefits in industry. In particular, in plane and axisymmetric jets, extensive investigations have been carried out by using active techniques for turbulence enhancement as well as suppression, but investigations using passive techniques are not as extensive. The main objective in jet turbulence control is to target and interfere with the organised vortical structures that are formed due to Kelvin–Helmholtz instability in the mixing layer. Tong and Warhaft [11] and Parker et al [8] obtained a significant reduction of turbulence intensity by placing a thin wire ring in the shear layer near the nozzle exit plane. The width of the shear layer was reduced and the spectra of velocity fluctuations indicated the suppression of organised large structures in the mixing layer of the jet. Stephens [9] and Stephens et al [10] used grids and honeycombs to completely cover the nozzle exit and obtained similar results. Burattini et al [2] suggested that the grids suppress the shear layer instability and damp the jet column instability. Another passive technique employed in a plane jet is to place a bluff body like a cylinder in the potential core and use the vortex shedding behind it as a feed back mechanism to control the shear layer instability [6, 3, 5, 1]. Antonini and Romano [1] disturbed a circular jet by placing a long, thin cylinder parallel to the nozzle exit plane and obtained an increase in mixing.

In jet turbulence control using a grid, apart from the influence of the mesh size and wire diameter of the grid, the circular edge is also likely to have an impact on the jet development. By using wire screens to partially cover the test section of a wind tunnel, Oguchi and Inoue [7] produced a mixing layer similar to that developing behind a splitter plate. Smoke flow visualisation indicated the presence of large scale structures downstream of the grid in the mixing layer. When a thin wire was attached to the screen edge, vortex shedding behind the wire also dominated the flow. Use of a narrow rectangular mesh or a small diameter disk grid yielded a wake. Spectra of velocity fluctuations in the wake produced by a rectangular screen (Zhou and Antonia [12]) clearly showed the presence of organised vortical structures even though

there was no primary vortex street. Hydrogen bubble flow visualisation (Finlay [4]) in the wake of a rectangular grid (Figure 1) shows the formation of large structures downstream.



Figure 1: Hydrogen bubble flow visualisation of structures behind a grid (from [4]).

The main aim of the present work is to investigate the effect of placing an annular grid and a disk grid at the nozzle exit plane on the development of a circular jet by using a single hot wire probe. The annular grid perturbs the initial shear layer and a small peripheral part of the potential core; the disk grid covers most of the potential core.

Experimental Conditions

The jet was produced by a 55 mm diameter (d) circular nozzle to which air was supplied by a variable speed centrifugal blower via a diffuser, settling chamber and contraction which had an area ratio of 85:1. Two annular and two disk grids were used in this

Case	Grid	Wire dia. (mm)	Aperture size (mm×mm)	Outer dia. (mm)	Inner dia. (mm)
1	Annular	0.5	1.25×1.25	100	30
2	Annular	0.2	0.54×0.54	100	30
3	Disk	0.5	1.25×1.25	30	–
4	Disk	0.2	0.54×0.54	30	–

Table 1: Summary of mesh geometry for disturbed flow conditions.

study and Table 1 gives the details of the grid geometry, mesh and wire size. Hereafter, measurement conditions will be referred to as Cases 1, 2, 3 and 4. The grid was isolated from the body of the jet by mounting it on a separate frame which was placed at a distance of 2 mm downstream of the nozzle exit plane. Figure 2 shows the nozzle, the coordinate axes and the four grids. Measurements of the mean velocity (U) and the longitudinal velocity fluctuation (u) were made by using a single hot wire probe operated in a constant temperature mode. The hot wire, made of 90% Pt-10% Rh, had diameter was 2.5 μm and the wire length to diameter ratio was nearly 200. A height gauge with a resolution of 0.01 mm was used to move the probe in the y -

direction. The hot wire signals were digitised using a 12 bit A/D converter and stored on a PC for further processing.

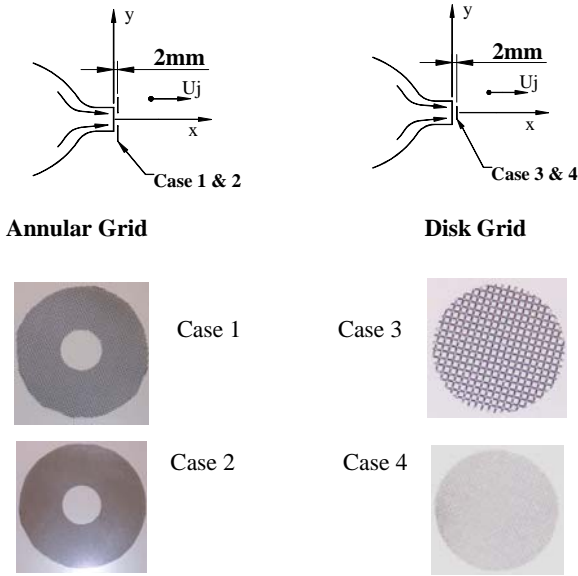


Figure 2: Co-ordinate system and grid configuration.

The jet exit velocity (U_j) was 10 m/s which yielded a Reynolds number $Re_d = 3.7 \times 10^4$. For the annular grid measurements, U_j was determined by placing a Pitot tube close to the nozzle exit plane in the potential core. For the disk grid, U_j was set at 10 m/s at $x/d = 2$ since the flow immediately downstream of the grid is unsteady due to the vortex shedding from the mesh. Burattini et al [2] also employed a similar approach to set U_j in their measurements behind a grid. Distributions of mean velocity (U) and rms velocity fluctuation (u') were obtained at several locations up to $x/d = 10$. The nozzle exit boundary layer was laminar and exhibited a small deviation from the Blasius profile. The shape factor was 2.2 which is smaller than the value of 2.59 for the Blasius distribution. The shear layer instability frequency f_0 (Kelvin – Helmholtz instability frequency) was approximately 600 Hz which yielded a Strouhal number $St_{\theta_0} (= f_0 \theta_0 / U_j, \theta_0$ is the nozzle boundary layer momentum thickness) = 0.013 which is in agreement with the values available in the literature.

Results and Discussion

Mean Velocity Distribution

The normalised mean velocity distributions U/U_j of the undisturbed jet and the jet with grids are shown in Figure 3 and 4 for $x/d = 0.2, 1, 2, 4, 6$ and 10 to include parts of the mixing layer and the transition zone of the jet. At $x/d = 2, 4, 6$ and 10 , the distributions with the annular mesh (Figure 3, Case 1) have a reduced lateral spread which is reflected in a smaller width of the shear layer which is consistent with the results of Burattini et al [2] and Stephens et al [10]. At $x/d = 0.2$ and 0.4 , U/U_j profiles exhibit a discontinuity with a rapid decrease between $y/d \approx 0.35$ and 0.5 . This region of a rapid change in U corresponds to the interphase between the potential core and the inner edge of the annular mesh which produces a mixing layer type of flow, somewhat similar to the two-stream mixing layer obtained by Oguchi and Inoue [7]. This layer disappears rapidly and cannot be identified for $x/d > 4$. The mean velocity gradient inside this layer is smaller for the grid with a finer mesh and wire size (Case 2) compared to Case 1 which implies that the fine mesh produces a rapid mixing and results in a reduced velocity gradient. Another possibility is that the width of the shear layer formed by the mesh is smaller for the fine grid compared to that for the coarse grid

(Case 1). For this flow at $x/d = 6$ and 10 , the value of U/U_j on the centreline is

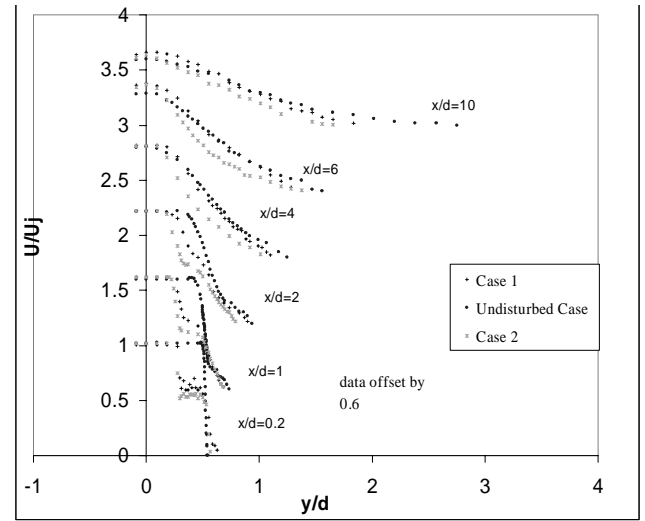


Figure 3: Mean velocity distribution with annular grids.

slightly larger than that of the undisturbed jet whereas for Case 2, there is a small excess at $x/d = 6$ which disappears at $x/d = 10$. This observation suggests that the influence of the coarse grid persists for a larger downstream distance compared to that of the fine grid. Distributions of U/U_j for the disk grids (Cases 3 and 4) indicate a negligible influence on the width of the jet while, in the potential core region, the mean velocity is smaller compared

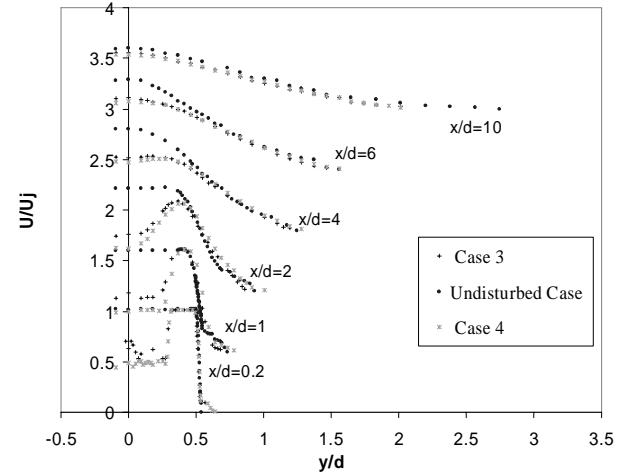


Figure 4: Mean velocity distribution with disk grids.

to the undisturbed jet (Figure 4). At $x/d = 0.2$, the mixing zone at the outer edge of the disk grid yields a rapid increase in U/U_j , which disappears for $x/d > 4$.

RMS Velocity Fluctuation u'

Distributions of u'/U_j at different downstream locations for the annular grid (Figure 5) show that these grids produce a significant amount of turbulence suppression. For example, at $x/d = 1$, the maximum value of u'/U_j is reduced by 60 % and 50 % respectively for Cases 1 and 2. Large reductions can be observed at other downstream locations also. A significant feature of u'/U_j distribution for the flows with annular grids is the presence of two maxima at $x/d = 1$ and 2 ; at other downstream locations, the peaks are still discernible. The peak at small y/d can be identified with the presence of the mixing zone produced by the inner edge of the mesh whereas the peak at large y/d is due to the jet mixing layer. Unlike the inner edge, the outer edge protrudes into the ambient region and does not produce a mixing zone. The grid with a finer mesh exhibits a peak in u'/U_j at the outer edge of the

jet (large y/d) compared to the coarse grid. The influence of both annular grids decreases as x/d increases.

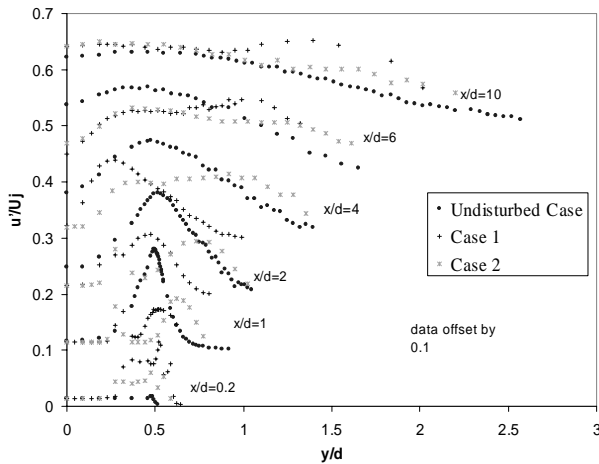


Figure 5: Distribution of rms velocity fluctuation with annular grids.

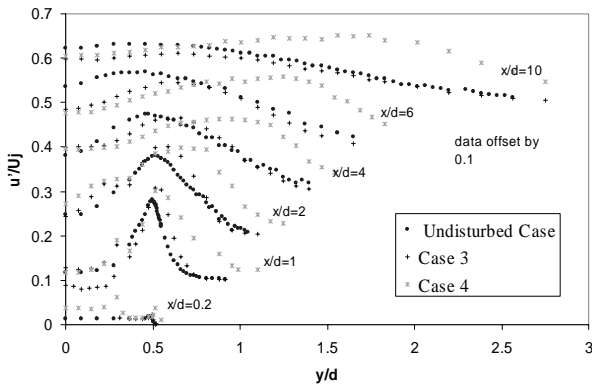


Figure 6: Distribution of rms velocity fluctuation with disk grids.

For the disk grids placed in the potential core (Cases 3 and 4), u'/U_j increases slightly at $x/d = 1$ and 2 (Figure 6). The distributions have two maxima – one associated with the mixing zone of the edge of the grid and the other inside the jet mixing layer. At $x/d = 4, 6$ and 10, the distributions exhibit a broad maxima. For the fine mesh disk (Case 4), the maxima occur at larger y/d values compared to the other two conditions. As x/d increases, the distribution for Case 4 deviates from those of the undisturbed and Case 3 flows. Antonini and Romano [1] also observed two peaks in u'/U_j distributions in their modified jet measurements. They observed an increase in u'/U_j and a lateral shift in the location of the maximum value compared to an undisturbed jet. In a plane jet disturbed by placing a cylinder in the potential core, Hsiao et al [6] observed an induced self sustaining oscillation at the cylinder vortex shedding frequency; in this flow, Chou et al [3] obtained an enhanced mixing. In a plane jet with a cylinder in the potential core, Henry et al [5] obtained a large amplitude peak in the mixing layer spectra at the cylinder vortex shedding frequency instead of the instability frequency, suggesting a resonant interaction between the jet exit and the cylinder vortex shedding. However, for this to occur, an intense vortex shedding from a relatively large diameter cylinder was necessary since small diameter cylinders produced only weak vortex shedding.

Centreline Distributions

Centreline distributions of U/U_j for the undisturbed and all the disturbed (Case 1–4) flows are shown in Figure 7. The annular

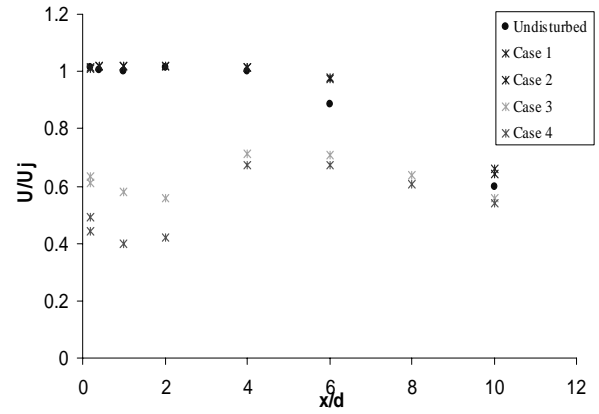


Figure 7: Centreline mean velocity distribution.

mesh extends the potential core to $x/d = 6$ from a value of 4 for the undisturbed jet which reflects a contraction of the shear layer for the jets with the annular mesh. The mesh and wire size have little influence on the centreline velocity. For the disk grids with a coarse mesh, U/U_j decreases slightly from a value of 0.6 (Case 3) up to $x/d = 2$ followed by an increase up to $x/d = 6$. Downstream of this location, U/U_j decreases continuously, similar to the undisturbed jet. For the disk with fine mesh (Case 4), centreline velocities are smaller, but the distribution has a shape similar to that of Case 3. The initial decrease in U_j up to $x/d = 2$ and 4, the increase in U_j might be linked to the growth of the jet which is associated with a reduction in the size of the central core. For the jet with the disk grids, it is not possible to identify a potential core in the conventional sense.

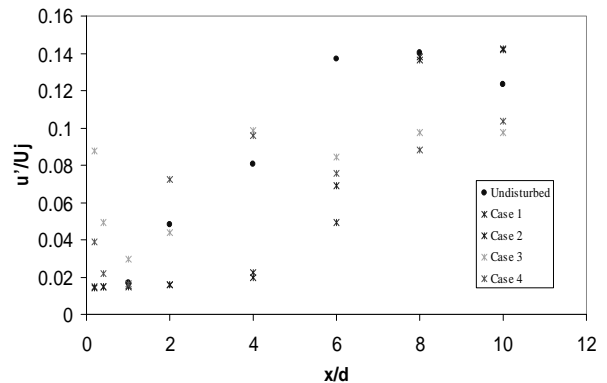


Figure 8: Centreline rms velocity fluctuation distribution.

For Cases 1 and 2, the centreline distributions of u'/U_j are almost identical (Figure 8), but are different to the distribution for the undisturbed jet. The maximum value of u'/U_j is nearly the same (14.5%) for the undisturbed and disturbed flows, but the maximum for the grid flows occurs at $x/d = 6$, compared to $x/d = 4$ for the undisturbed jet. This result provides additional support for the extension of the potential core. The two disk meshes also produce almost identical centreline distributions of u'/U_j , with a local minimum at $x/d = 1$ followed by a maximum at $x/d = 4$.

Spectra of u

For the undisturbed jet, u spectra at $x/d = 0.2$ and 0.4 and $y/d = 0.5$, which is in line with the nozzle tip (Figure 9), indicate the presence of organised large structures at the instability frequency of approximately 600 Hz.

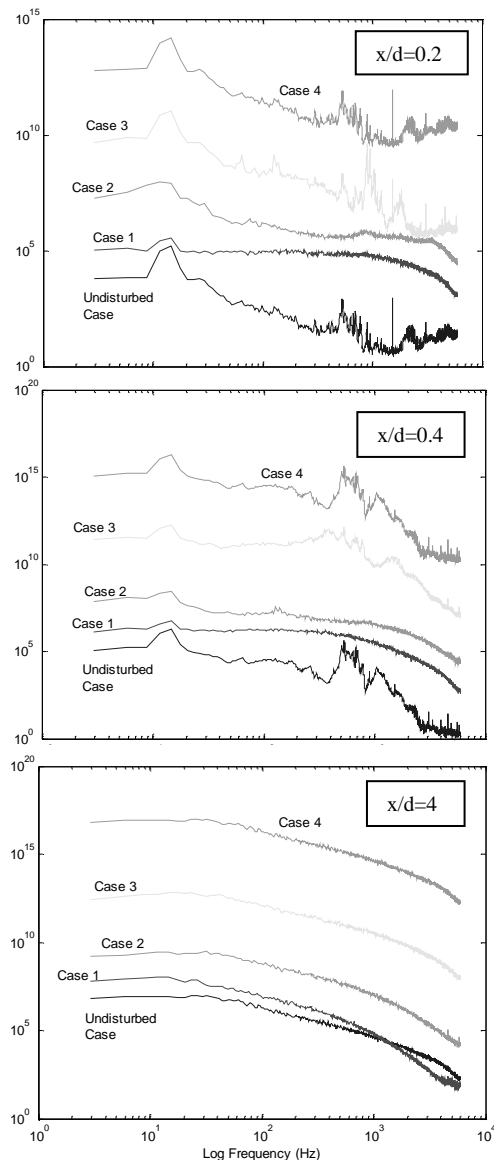


Figure 9: Spectra of u' with annular and mesh grids.

With the annular grids in place, the spectral peak at this frequency cannot be identified, indicating that the grids suppress the formation of organised vortical structures near the nozzle exit. This result is similar to that of Burattini et al [2] and Stephens et al [10] when the jet nozzle was completely covered by grid and honeycomb. Lack of organised structures results in a reduced growth rate and a smaller shear layer width. At $x/d = 4$, the spectra for the undisturbed flow and Cases 1 and 2 are almost identical and the lack of spectral peaks indicates the absence of an organised motion. The disk grids have no influence on the formation of organised structures at $x/d = 0.2$ and the spectral peak near 600 Hz can be identified for the undisturbed and the grid flows. However, at $x/d = 0.4$, additional peaks can be seen in the spectra for these grids (Cases 3 and 4). The additional peaks may be associated with the shear layer produced at the edge of the disk grid, but further investigation is needed to confirm this. At $x/d = 4$, all the three spectra are almost identical.

Conclusions

The two annular grids used in this investigation suppress the formation of the shear layer (Kelvin-Helmholtz) instability and

inhibit the formation of organised vortical structures. This leads to a reduction in the growth rate and an extension of the length of the potential core. The mean velocity distributions close to the nozzle exit exhibit a discontinuity which can be identified with the mixing zone formed at the inner edge of the grid. Distributions of u' exhibit two peaks, one of which is inside the jet mixing layer whilst the other one occurs closer to the jet axis, due to the mixing (shear) zone mentioned previously. The absence of a spectral peak confirms the suppression of the organised motion in the jet mixing layer. The disk grids have negligible influence on the development of the jet. The organised vortices are not suppressed and the growth rate of the undisturbed and disturbed jets is nearly the same. The value of u' was slightly larger compared to the undisturbed jet which yields an enhanced mixing. Similar to the annular grid, the distributions of U exhibit a discontinuity and u' distributions exhibit two peaks. These observations are related to the mixing zone formed at the outer edge of the disk which is inside the potential core. Both the annular grids and disk grids have potential in the context of jet turbulence control. The disk grid increases the turbulence level which yields an enhanced mixing. On the other hand, the annular grid suppresses turbulence which is also achieved by a full grid. However, the annular grid produces a smaller pressure drop at the exit compared to a full grid.

References

- [1] Antonini, I. and Romano, G.P., Passive Control of the Turbulent Flow at the Outlet of a Circular Jet by Means of a Cylinder, *Turbulent Shear Flow Phenomena -2*, editors E. Lindborg, A. Johansson, J. Eaton, J. Humphrey, N. Kasagi, M. Leschziner, & M. Somersfeld, 2001, Sweden.
- [2] Burattini, P., Antonia, R.A., Rajagopalan, S. and Stephens, M., Effect of Initial Conditions on the Near Field Development of a Round Jet, *Exp. Fluids*, **37**, 2004, 56-64.
- [3] Chou, Y-W., Hsiao, F-B., Hsu, C-C. and Huang, J-M., Vortex Dynamics and Energy Transport of a Plane Jet Impinging Upon a Small Cylinder, *Exp. Thermal Fluid Sci.*, **26**, 2002, 445-454.
- [4] Finlay, S., *Development of Flow Visualisation Facilities*, B.E. Thesis, University of Newcastle, 1999.
- [5] Henry, P., Olsen, J. and Rajagopalan, S., Passive Control of the Shear layer Turbulence in a Plane Jet, *Proc. 8th Asian Congress of Fluid Mechanics*, editor E. Cui, Shenzhen, China, 1999, 559-562.
- [6] Hsiao, F-B., Chou, Y.-W. and Huang, J-M., The Study of Self-Sustained Oscillating Plane Jet Flow Impinging Upon a Small Cylinder, *Exp. Fluids*, **27**, 1999, 392-399.
- [7] Oguchi, H. and Inoue, O., Mixing Layer Produced by a Screen and its Dependence on Initial Condition, *J. Fluid Mech.*, **142**, 1984, 217-231.
- [8] Parker, R., Rajagopalan, S. and Antonia, R.A., Control of an Axisymmetric Jet Using a Passive Ring, *Proc. Fourteenth Australasian Fluid Mechanics Conference*, editor B. Dalley, 2001, Adelaide.
- [9] Stephens, M., *Axisymmetric Shear Layer Behind a Grid*, B.E. Thesis, University of Newcastle, 2002.
- [10] Stephens, M., Rajagopalan, S., Burattini, P. and Antonia, R.A., Axisymmetric Shear Flow Behind a Honeycomb, *Proc. Tenth Asian Congress of Fluid Mechanics*, editor J.J. Wijetunge, 2004, Sri Lanka, Paper No. D16.
- [11] Tong, C. and Warhaft, Z., Turbulence Suppression in a Jet by Means of a Fine Ring, *Phys. Fluids*, **6**, 1994, 328-333
- [12] Zhou, Y. and Antonia, R.A., Memory Effects in a Plane Turbulent Wake, *Exp. Fluids*, **19**, 1995, 112-120.